Investigation of Plasmonic Resonances in Mismatched Gold Nanocone Dimers

Adnan Daud Khan · Giovanni Miano

Abstract The plasmonic properties of two closely adjacent gold nanocones of different sizes have been investigated. The plasmon modes of the first nanocone couple with the plasmon modes of the second one due to which a broad peak and a narrow peak emerges in the extinction spectrum, which can be categorized as bright and dark plasmon modes. The destructive interference of the two modes results in a sharp Fano dip in the spectrum. Several configurations of the conical nanodimer have been considered, which suggests that the plasmon coupling in the nanocone dimer is not only dependent on the interparticle distance and size of the nanoparticles but also on their spatial arrangement. The localized high near-field energy in the nanodimer can be used for surface-enhanced Raman spectroscopy applications.

Keywords Dimers · Fano resonance · Plasmons · Nanocones · Near-field enhancement

Introduction

Surface plasmons of metal nanoparticles are able to produce very strong and confined optical fields at deep subwavelength volumes, far beyond the diffraction limit. When the two metal nanoparticles are placed closed to each other to make a dimer, their optical properties are highly changed because the plasmon modes of both the metals couple together and form new hybridized plasmon modes. By decreasing the gap between the two nanoparticles, the plasmon coupling of the nanoparticles

A. D. Khan · G. Miano (✉)
Department of Electrical Engineering, University of Naples
"Federico II", via Claudio 21, 80125 Naples, Italy
e-mail: miano@unina.it

A. D. Khan
e-mail: adnandaud.khan@unina.it

increases, which results in the amplification of the field intensity by orders of magnitude. Because of this property, the dimer nanostructure has received a huge attention for surface-enhanced Raman spectroscopy (SERS) applications due to the hot spot produced in the gap between the nanoparticles when incident light is polarized along the dimer axis [1–4].

Recently, it has been established that the plasmonic dimer nanostructure also supports Fano like resonances [3, 5–10]. The Fano resonances usually crop up from the coupling and interference of a non-radiative mode (dark mode) and a continuum (bright mode) of radiative electromagnetic waves and are distinguished from their Lorentzian counterpart by a distinctive asymmetric line shape. They are typically more sensitive to the shapes of the nanoparticles and changes of the refractive index of the environment. Various geometries based on dimer structures have been proposed to achieve Fano resonances. Brown et al. have experimentally and theoretically analyzed mismatched nanoparticle pairs of different size and shapes, which give rise to properties such as Fano resonances, avoided crossing behavior, and optical nanodiode effect [8]. Yang et al. have theoretically investigated the plasmon coupling in metallic nanorod dimers. They observed a pronounced dip in the optical spectrum due to plasmonic Fano resonance which is induced by destructive interference between bright dipole mode of the short nanorod and dark quadrupole mode of the long nanorod [6]. Wu et al. have reported Fano-like resonances in the absorption spectrum of an asymmetric homodimer of gold elliptical nanowires, which arises from the coherent coupling between the superradiant bright mode and the subradiant dark mode [9]. Wu et al. have also demonstrated the influence of symmetry breaking on the plasmon resonance coupling in the gold nanotube dimer and observed strong Fano-like resonance in the scattering spectrum due to the interference of the bonding octopole mode of the dimer with the dipole modes [3]. Recently, Zheng et al. have observed Fano resonance in a T-shaped dimer, which arises

from the interference of the bright mode of the short nano-particle and the dark mode of the long nanoparticle [11].

We present here for the first time the observation of Fano resonance in a dimer based on mismatched gold nanocones, which are highly polarization-dependent nanostructures [12, 13]. In the asymmetric plasmonic nanodimer, the interactions between the modes having a distinct angular momenta or line shape are stronger. Unlike to homodimer, these symmetry-reduced nanostructures avoid crossings of the plasmon modes, provide a very sharp Fano resonance in the optical spectrum [8], and exhibit better sensitivities than the symmetric counterparts [14]. The Fano resonance observed in the mismatched conical nanodimer can be tuned and enhanced by modifying the size of one of the nanoparticle or the distance between the two nanocones. Here, we illustrate the results for the dimer separations only down to 1 nm because for smaller separations, the quantum mechanical effects, such as electron tunneling across the dimer junction and screening, alter the classical response [15].

Polarization control at nanoscale is an upcoming direction in the research of metamaterials. Due to the polarization sensitivity of the proposed nanodimer, we have different response for transverse and longitudinal polarizations, therefore the nanodimer can be used as polarization beam filter [16]. Furthermore, we have spectral line shapes with strong Fano resonances, which is an essential feature for having highly dispersive metamaterials. The dispersion engineering in metamaterials is typically done through asymmetric spectral line shape with steep variations. In this paper, we investigate several configurations of cone-based dimers with special emphasis on the spectral line shape. We found some configurations that seem very useful for Fano spectral line shape and near-field enhancement. Polarization control and strong asymmetric spectral line shape make the proposed nanodimer an ideal candidate to be used in the applications like plasmon-induced transparency (PIT), switching, and SERS.

The optical properties of the dimer nanostructures are carried out by COMSOL with RF module. Johnson and Christy data have been used for the dielectric constant of the gold [17]. The embedding medium is considered air.
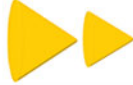
Optical Properties of the Nanocone Dimer

In this paper, we analyze different configurations of the dimer nanostructure, see Table 1.

Type I Nanodimer

Figure 1 shows the schematic diagram of a type I heterodimer. The dimensions of the nanodimer are R_1, H_1/R_2, and H_2, where 'R_1' and 'H_1' are the radius and height of the large

Table 1 Several configurations of a conical nanodimer

nanocone, and 'R_2' and 'H_2' are the radius and height of the small nanocone, respectively. The gap size between the two nanocones is denoted with 'G'. The illuminating electromagnetic wave is linearly polarized, the electric field is directed along x-direction, and the wave propagates in the y-direction.

We analyze first the extinction spectra of the dimer composed of two nanocones with dimensions; R_1, H_1=90, 110 and R_2, H_2=50, 70 nm, respectively. Figure 2a shows the extinction spectra of the single nanocones, when they do not interact. The large nanocone exhibits a sharp extinction peak near 638 nm while the small one at 552 nm. Both the peaks are relevant to the fundamental dipole mode. Now, when the two nanocones are brought close enough to form a dimer (type I), the plasmon modes of the first nanocone couple primarily with the plasmon modes of the second one due to which a low-energy bonding mode, and a high-energy anti-bonding mode are formed according to the plasmon hybridization model [18]. The antibonding mode cannot be visualized in the spectrum due to its extremely small dipole moment, so only the bonding mode emerges in the spectrum due to its large dipole moment [18, 19]. Since the dimer is mismatched, the dipole mode of the small nanocone interacts with the dipole and higher order modes of the large nanocone forming hybridized dipole–dipole (DDB), dipole–quadrupole (DQB), and dipole–multipolar bonding modes [7, 8]. Figure 2b shows the extinction spectra of the dimer with a gap of G=1 nm. It shows a mixture of the hybridized bright DDB mode near 770 nm and the dark DQB mode near 630 nm. The higher energy peak is much weaker than the lower energy one. The two modes overlap in energy and induce a sharp Fano resonance in the visible range near 682 nm, which is characterized by a dip in the spectrum. From the blue and red curves corresponding to the two arrangements shown in the inset of Fig. 2b, swapping the nanocones does not affect significantly the extinction
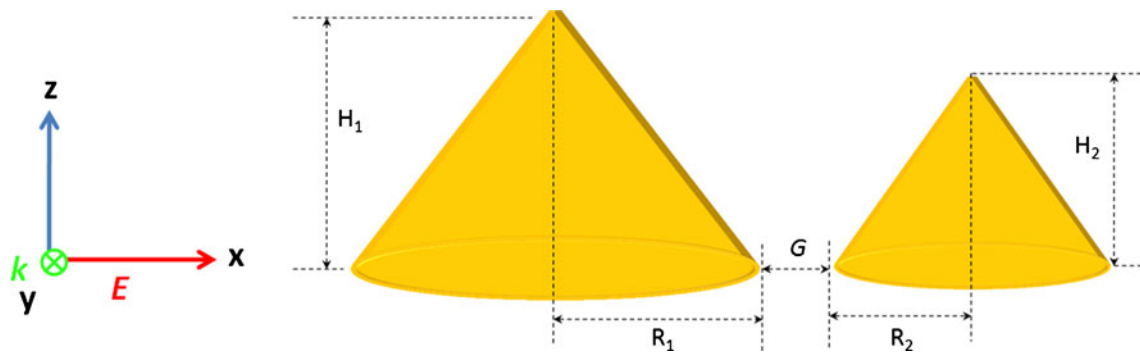
Fig. 1 Sketch of the dimer nanostructure. The incident field is linearly polarized along the *x*-direction and propagates along the *y*-direction

spectra of the nanodimer. The surface charge distributions (top view) corresponding to each peak and Fano dip are shown in the inset of Fig. 2b. The surface charges near 770 nm shows a dipole distribution on both the nanoparticles, which clearly represents a DDB mode. The surface charges near 630 nm shows a quadrupolar-like distribution on both the nanoparticles, depicting a DQB mode, while the surface charges at the dip shows a mixture of dipole and quadrupole modes.

The polarization state of the incident light also has a great effect on the extinction spectra of the dimer. Figure 3 shows the extinction spectra of the dimer with both the longitudinal (blue line) and transverse (red line) excitations at fixed $G=1$ nm. For a transverse polarized incident light, the electrostatic coupling between the nanoparticles is predicted to be of less significance. Here, the field enhancement and plasmon coupling are very weak compared to the
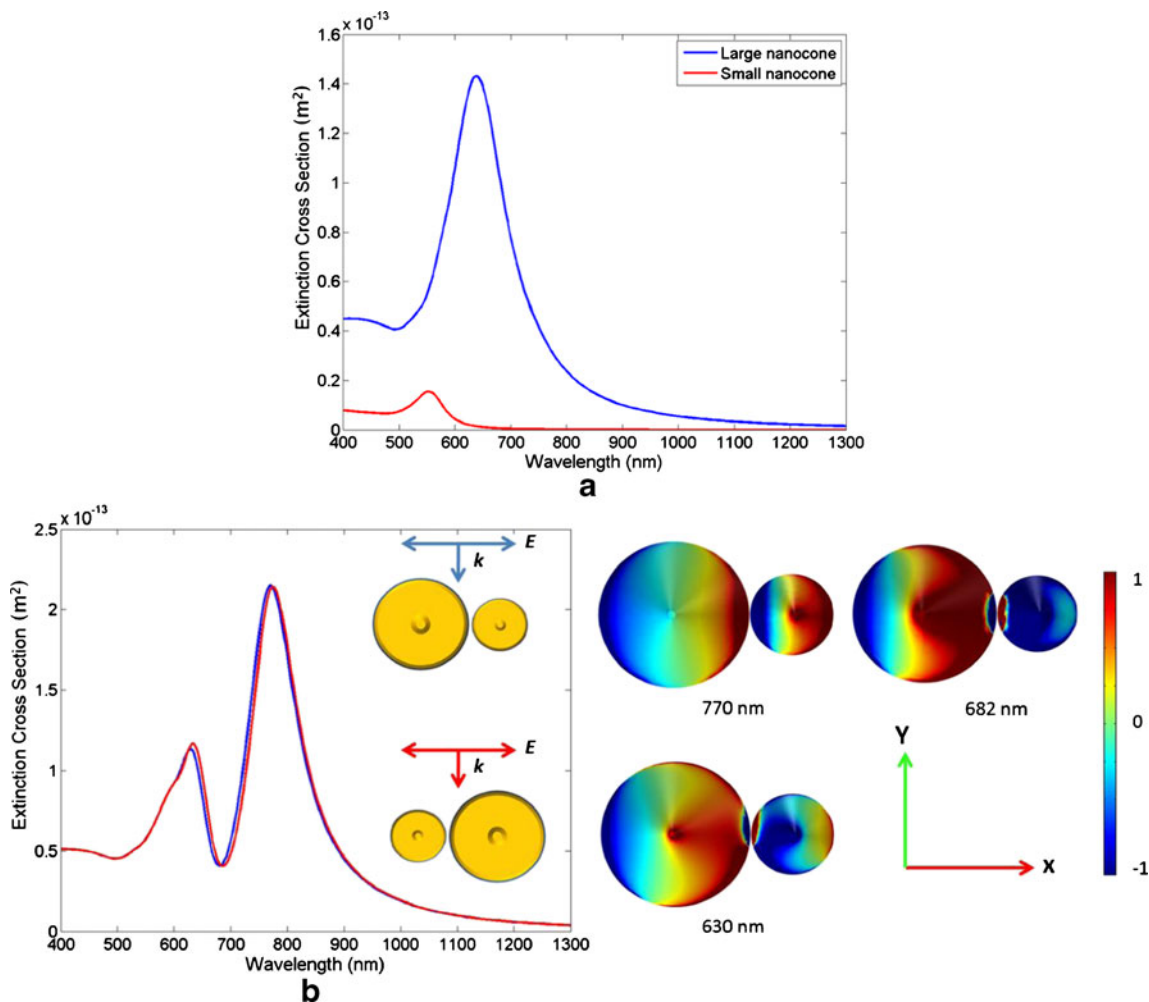

Fig. 2 Extinction spectra of **a** single large and small nanocones **b** type I nanodimer. Inset shows surface charge distributions
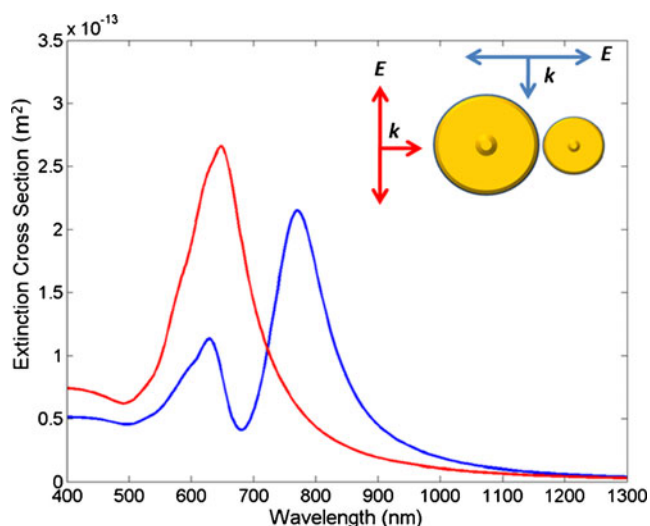
Fig. 3 Extinction spectra of a type I nanodimer with longitudinal (*blue*) and transverse (*red*) polarizations

longitudinal excitation because the hybridization effects are limited [8, 19]. So, for the transverse polarization, the Fano dip disappears, and we observed only a single dipole peak near 650 nm. The higher order hybridized modes remain absent in this case, and the dimer acts as a monomer. Thus, by changing the polarization of incident field, the Fano resonance can be switched on and off.

Figure 4 demonstrates the extinction spectra of a type I nanodimer with different values of G. When the gap is small, then the plasmon interactions between the two nanocones increases, which results in the red shifting of the plasmonic peaks. For instance, by decreasing the value of G from 7 to 1 nm, an obvious red shift of both the DDB and DQB modes occur. It is further to be noted that by increasing the value of
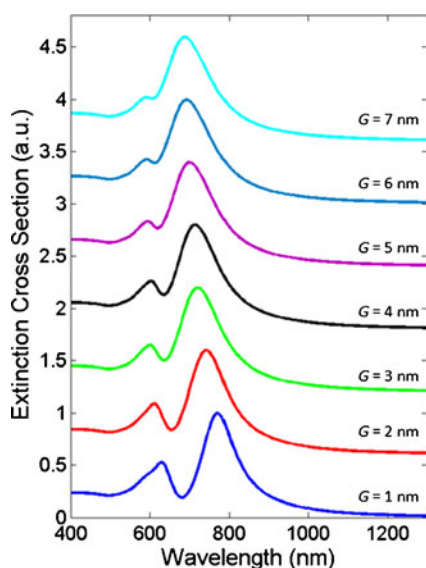

Fig. 4 Extinction spectra of a nanodimer for different values of G

G, the DQB mode gets weaker, while the DDB mode becomes stronger, which results in the weakening of Fano resonance. For a very large value of G, the plasmon hybridization between the two nanocones are reduced due to which the dimer which acts as an isolated monomer because only a single resonance dominates the extinction spectrum, and no Fano resonance can be perceived.

Figure 5a shows the extinction spectra of a type I dimer by modifying the dimensions of the first nanocone at fix $G=1$ nm, in which the intensity and the spectral position of both resonances vary. It appears that as R_1 and H_1 get smaller, the DDB mode becomes narrow band because of the decrease in the polarizability of the first nanocone. Also, the Fano resonance is comparatively weak for smaller values of R_1 and H_1. Figure 5b gives the resonant wavelengths of the DDB and DQB modes as the dimensions of the first nanocone varies (keeping same aspect ratio) at fix $G=1$ nm. Both the DDB and DQB modes gradually red shift as R_1 and H_1 increases, but the red shift of the DQB mode is very weak compared to DDB mode. So by summarizing, the spectral location and modulation depth of the Fano resonance can be controlled by modifying G or the size of the nanoparticle.

We named the dimer with dimensions 30,50/50,70 nm as type IA and the dimer with dimensions 90,110/50,70 nm as type IB nanodimer. Figure 6 shows the distribution of the real part of the electric field of type IB nanodimer at different wavelengths. The maximum value of the enhancement is observed in the gap region between the two nanoparticles. The field distributions are relevant to the DDB and DQB modes as well as a Fano resonance [20, 21]. For the type IB nanodimer, the maximum value of the field enhancement for the DDB mode is found to be 245 and that for the DQB mode is 330. For the type IA nanodimer, the maximum value of the enhancement for the DDB mode is 400 and that for the DQB mode is 260, which are reasonably higher than the type IB nanodimer. So, in this configuration of a nanodimer, the type IB exhibit strong Fano resonance, which may be useful for PIT [22], whereas the type IA provides large field enhancement, which is an important feature of SERS [23, 24].

Type II Nanodimer

Next, we investigate the optical properties of type II nanodimer. Here, the tips of both the nanocones are in the same direction as shown in Fig. 7a. Figure 7b shows the extinction spectra of type II nanodimer for different values of R_1 and H_1 at fixed $G=1$ nm. The results obtained for this type is quite different from the type I configuration. Here, by decreasing the value of R_1 and H_1, the spectral width and position of the DDB and DQB modes changes, and also the separation between them starts to decrease. When the first nanocone size reaches to $R_1=30$ nm and $H_1=50$ nm, the DDB

Fig. 5 Extinction spectra of type I nanodimer for **a** different value of R_1 and H_1. **b** Wavelength shift as a function of R_1 for constant aspect ratio of the nanocone

a

b
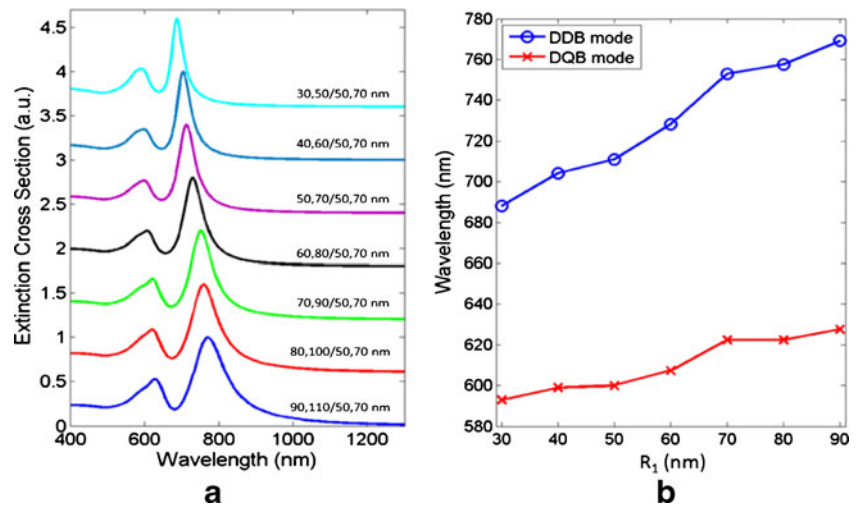
mode loses its strength and becomes narrow, while on the other hand the DQB mode gained enough strength and became broad due to which a Fano resonance with sharp modulation depth is observed in the spectrum. This Fano resonance was weak in the type IA nanodimer. We named the nanodimer with such dimensions as type IIA and the dimer with dimensions 90,110/50,70 nm as type IIB. The surface charge distribution corresponding to the two extinction peaks for type IIA nanodimer is shown in the inset. The peak near 655 nm corresponds to DDB mode, while the peak near 550 nm shows a quadrupolar-like pattern. Here, at the narrow gap between the two nanocones, the transfer of the charges occurs. For instance, the negative charges of the large nanocone migrate to small nanocone, and the positive charges of the small nanocone migrate to large nanocone, where the nature of this mode appears as quadrupolar. Figure 7c shows the wavelength shift of both the DDB and DQB modes as a function of R_1 at fixed $G=1$ nm. The DDB mode (blue line) shows a stronger shift towards the red compared to DQB mode. This shows that by reducing the size of the first nanocone, the DDB mode strongly blueshift, while the DQB mode has essentially retained its spectral location.

Figure 8a, b shows the extinction spectra of type IIB and IIA nanodimers for different values of G. It appears that by increasing the value of G, the DDB mode blueshifted, and the strength of the Fano resonance decreases. For high value of G, the double peak spectral feature vanishes, and no Fano resonance is observed in both the types. This situation is different from the type I nanodimer, where for high values of G, the Fano resonance still exist. So the type I nanodimer has the potential to exhibit strong Fano resonances in the extinction spectrum even for high value of G. However, the type IIA nanodimer has shown striking feature due to the appearance of intense Fano resonance for $G=1$ nm.

Figure 9 shows the distribution of the real part of the electric field of type IIB nanodimer for the DDB and DQB modes and Fano resonance at fixed $G=1$ nm. The field distributions reveal high values of the enhancement at the narrow gap between the two nanocones. For the type IIA nanodimer, the maximum value of the enhancement for the DDB mode is 255, while that of the DQB mode is 100. For the type IIB nanodimer, the maximum value for the DDB mode is observed to be 86, while that for the DQB mode is 46. So in this configuration, the type IIA nanodimer can be a
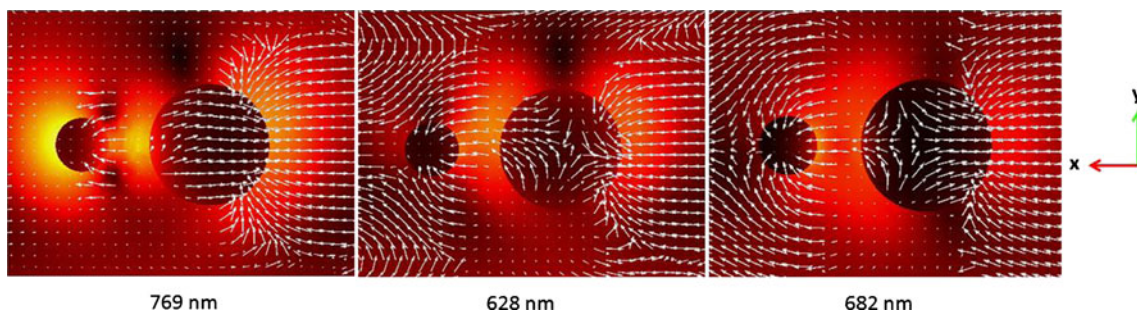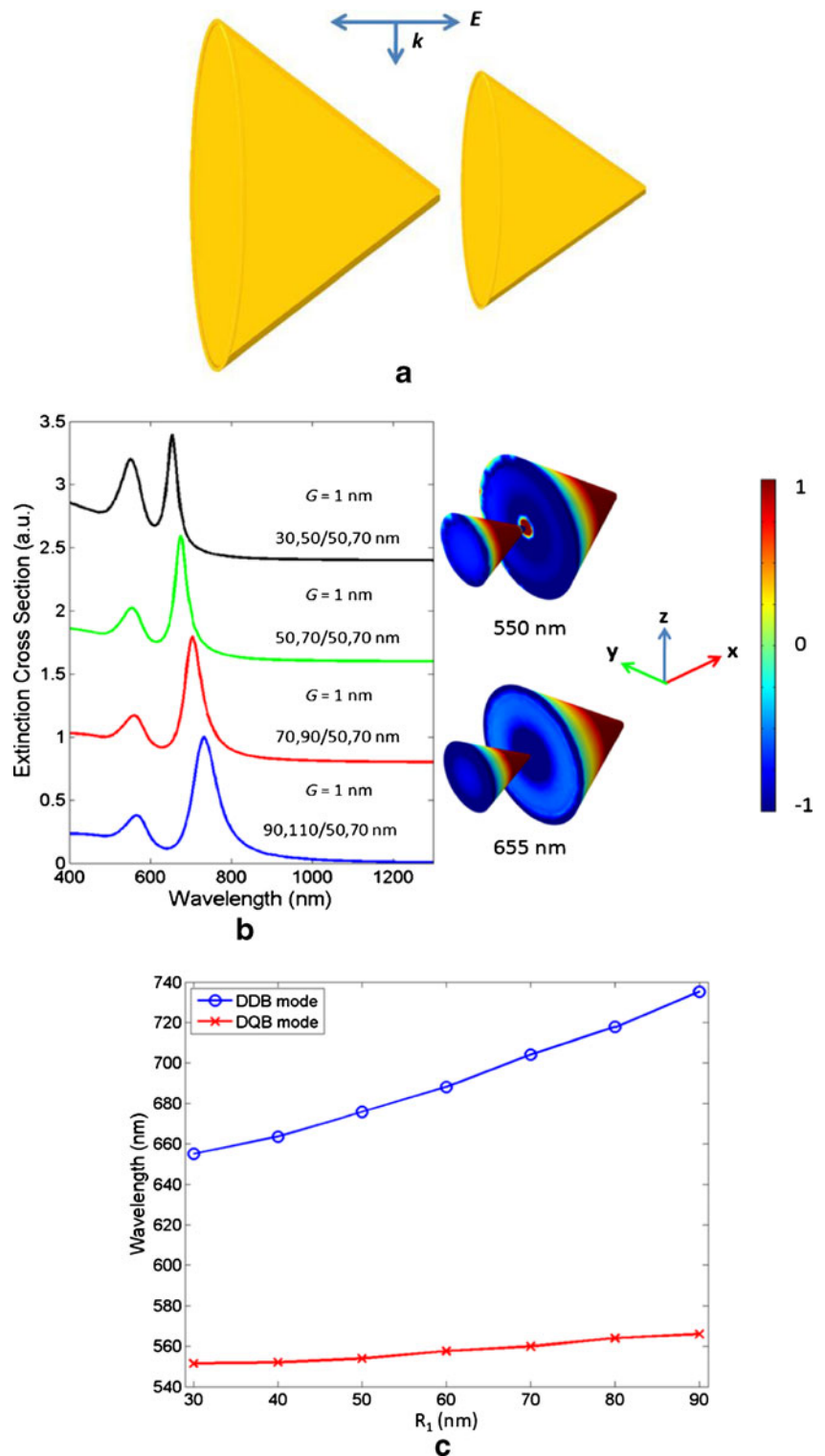

Fig. 6 Distributions of the real part of the electric field in the x–y-plane (z=0) of type IB nanodimer for the DDB and DQB modes and Fano resonance

Fig. 7 a Sketch of type II nanodimer. **b** Extinction cross-section of type II nanodimer. Insets show surface charge distributions. **c** Wavelength shift as a function of R_1 for constant aspect ratio of the nanocone


a

b

c

better choice for both the PIT and SERS applications [22, 24]. From the field distributions, it also becomes clear that, whatever the arrangement of the nanoparticles, the maximum near-field enhancement always takes place at the junction between the two nanoparticles by forming a so-called "hot spot."

Type III Nanodimer

In this section, we investigate the optical properties of type III nanodimer, where we place the tips of both the nanocones in front of each other as shown in Fig. 10a. Figure 10b shows the extinction spectra of the type III nanodimer. In this

Fig. 8 Extinction spectra of **a** type IIB and **b** type IIA nanodimers for different values of *G*
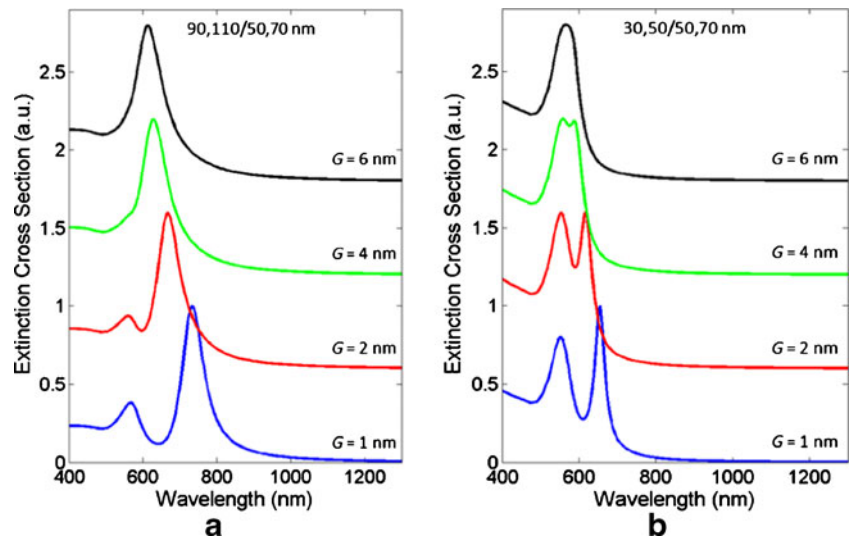
configuration, by decreasing the size of the first nanocone, an extremely small movement of the DDB mode occurs, and also the Fano resonance obtained in this case is very weak compared to the previous two cases. So the type III configuration is producing only weak Fano resonances. Figure 10c shows the wavelength shift as a function of R_1. It appears that by increasing the value of R_1, the DDB mode slightly red shift, while the DQB mode remains almost at the same position. This suggests that in the type III configuration, the Fano resonance and the hybridized modes are not very sensitive to the size of the nanoparticle unlike the previous two types.

Figure 11 shows the extinction spectrum of the type III nanodimer with different dimensions for various values of *G*. The dimer with dimensions 30,50/50,70 and 90,110/50,70 nm are named as type IIIA and type IIIB, respectively. In both the type IIIA and IIIB nanodimers, the blueshifting of the DDB mode is similar to the previous discussed cases, but no pronounced Fano resonance is observed. So, for the type III nanodimer, changing the gap *G* or the parameters of the nanoparticle do not yield strong Fano resonance.

The type III configuration of a conical nanodimer when the two nanoparticles are equal is also known under the name "bowtie nanoantenna," whose extinction spectra are shown by the green line in Fig. 10b. The extinction peaks of the bowtie nanoantenna can be tuned by varying the gap spacing and *b*-semi axis of the two nanocones (Fig. 12a). Figure 12b shows the case of varying *b* due to the DDB mode which red shifts from around 720 to 925 nm. Figure 12c shows the red shifting of the resonant modes as a function of *G*, where a large red shift is observed for the DDB mode. So the resonant peaks of the antenna can be tuned over a wide range, which can be used for highly sensitive biosensors [25, 26].

Figure 13 shows the distribution of the real part of the electric field for type IIIB nanodimer relevant to the DDB and DQB modes and Fano resonance. The highest value of the enhancement for type IIIA nanodimer is observed to be 180 for the DDB mode while that for the DQB mode is 60. On the other hand, for the type IIIB nanodimer, the maximum value of the enhancement for the DDB mode is 150 while that for the DQB mode is 87. These values of the enhancement are less than the previous two nanodimer types. Therefore, we can say that the type III nanodimer is not so
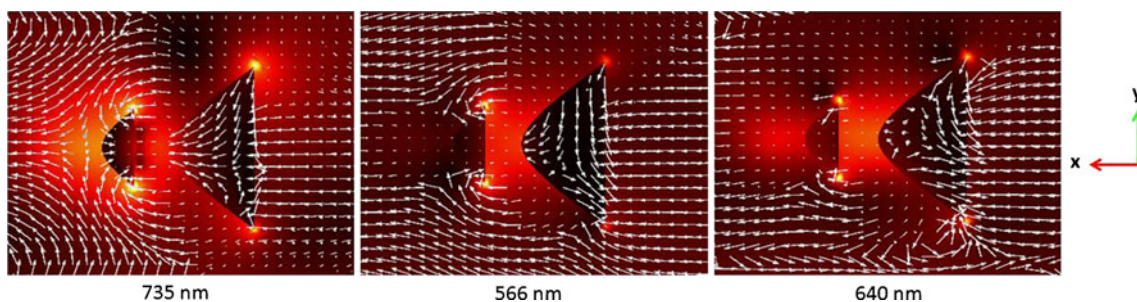

Fig. 9 Distributions of the real part of the electric field in the *x*–*y*-plane (*z*=0) of type IIB nanodimer for the DDB and DQB modes and Fano resonance

Fig. 10 **a** Sketch of type III nanodimer. **b** Extinction cross-section of type III nanodimer. **c** Wavelength shift as a function of R_1
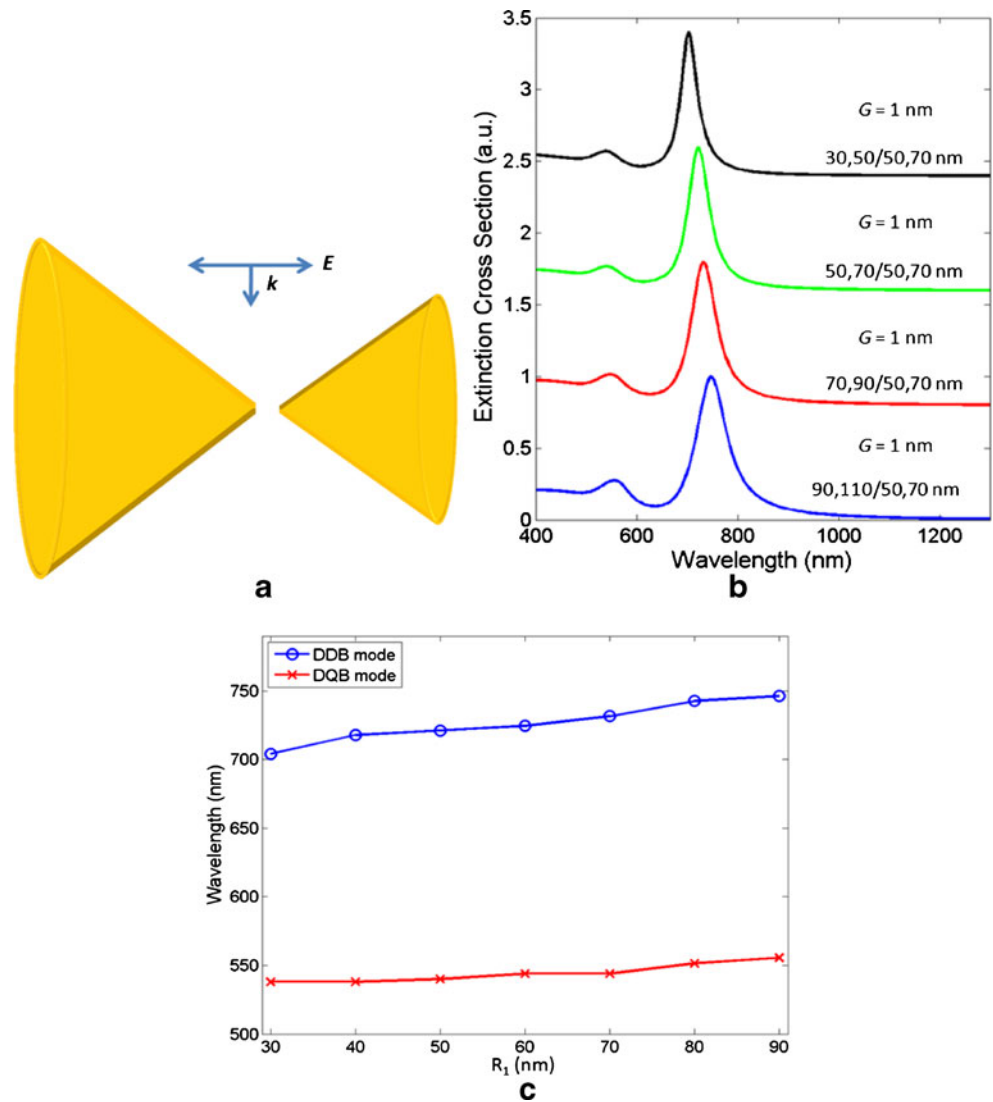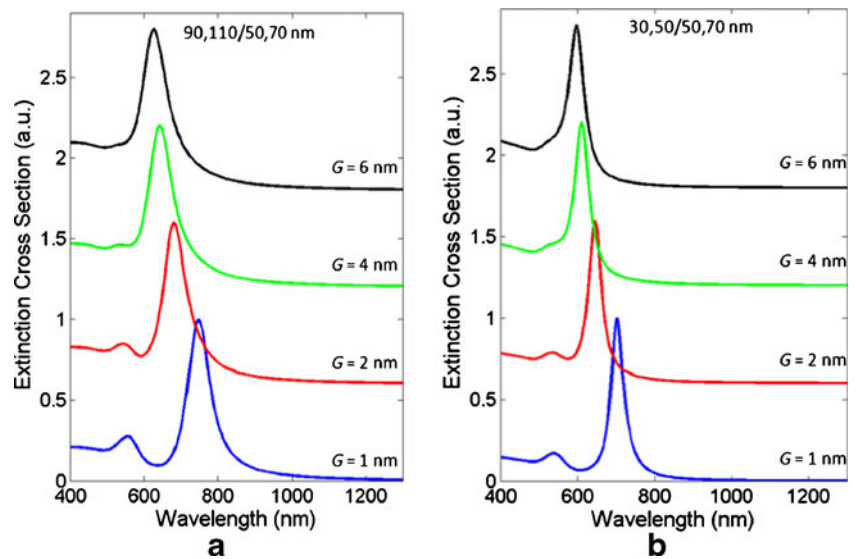

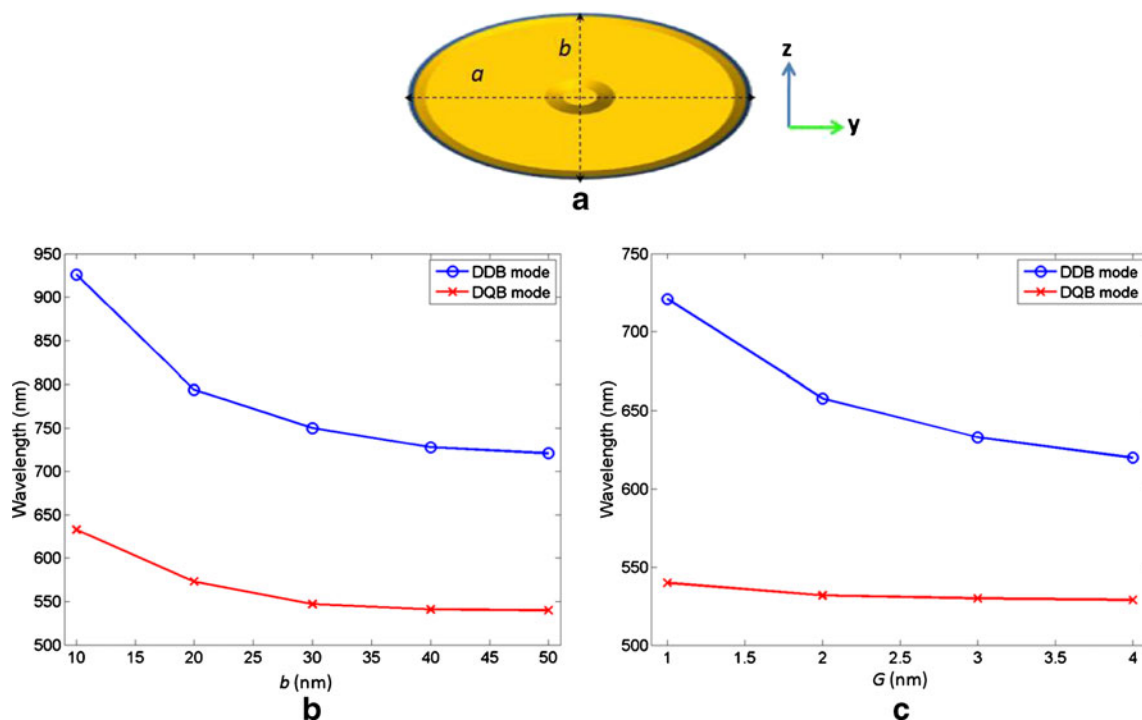**Fig. 11** Extinction spectra of **a** type IIIB and **b** type IIIA nanodimers for different values of G

Fig. 12 Nanocones with elliptical cross-section (**a**). Wavelength shift as function of **b** *b* and **c** *G*

proficient for high performance SERS. The near-field enhancement distributions of type I, II, and III nanodimers show that the lower-energy DDB mode will always exhibit large value of the enhancement like in the previous reported studies [3, 7, 27]. However, the type IB nanodimer shows a maximum value of the enhancement for the DQB mode, which is different from the other cases.

Type IV Nanodimer

Finally, we studied the optical properties of type IV nanodimer, where we placed the tips of both the nanocones in the opposite direction as shown in Fig. 14a. Figure 14b shows the extinction spectra of the type IV nanodimer, which is entirely different from the previously discussed

cases. Here, for all the values of R_1 and H_1, the extinction spectrum is dominated by the DDB mode, and only a slight peak at the lower energy level is observed. This peak is far ahead from the DDB mode where no coupling between the two modes will takes place. By reducing the size of the first nanocone, no distinct Fano profile is observed in the extinction spectrum because the two peaks are not close spectrally. However, by changing the interparticle gap, it is surprising to see that the two peaks come closer, overlap in energy, and induces a Fano resonance with a weak modulation depth. This situation is quite apparent for the type IVB (90,110/50,70 nm) nanodimer at $G=6$ nm, whose extinction cross-section is shown in Fig. 14c. This implies that the type IV nanodimer exhibits a remarkable sensitivity to the gap region.
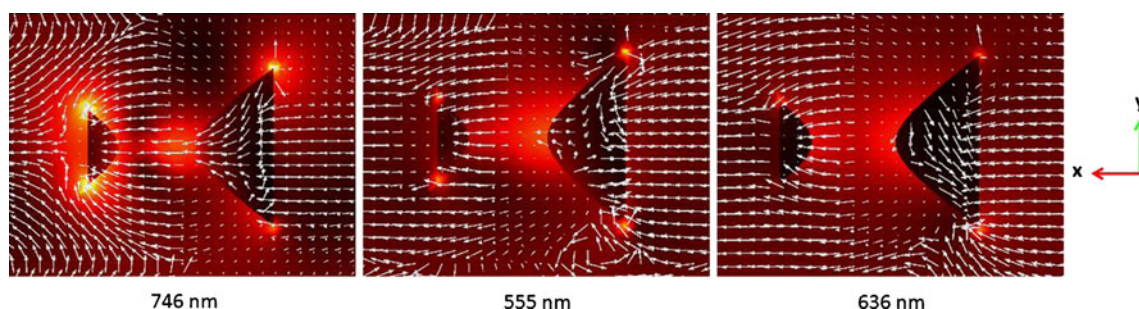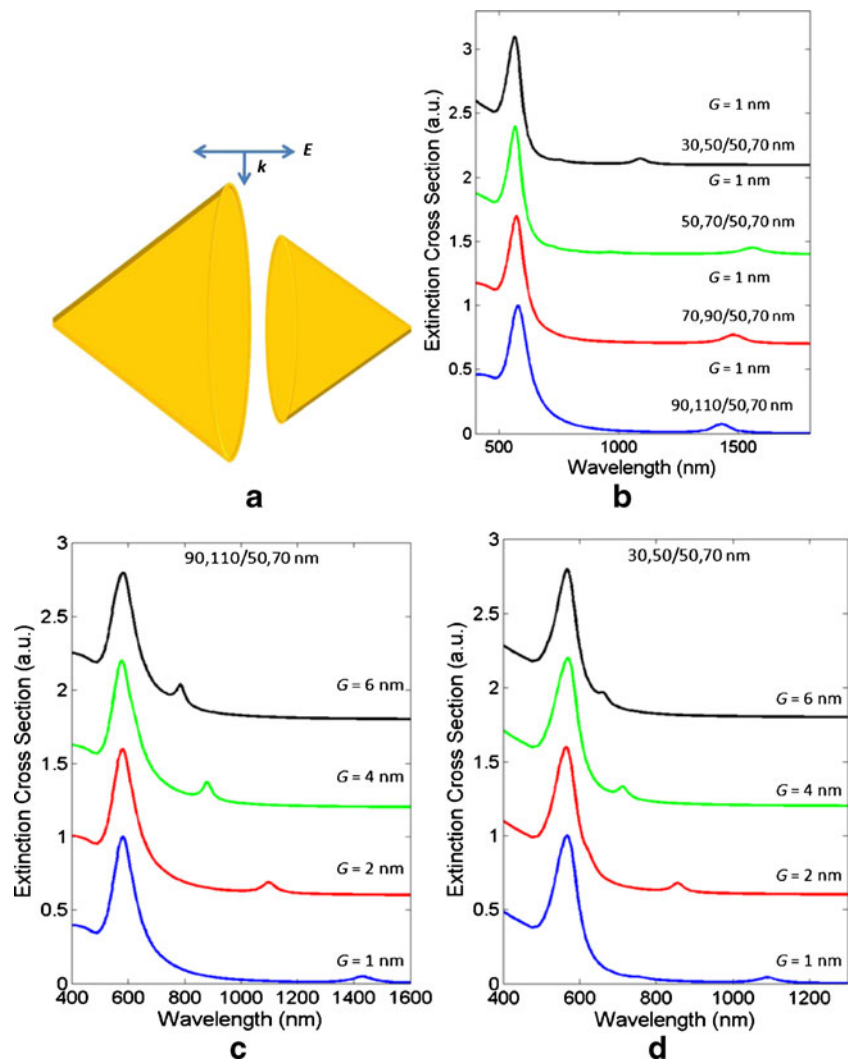

Fig. 13 Distributions of the real part of the electric field in the *x*–*y*-plane (*z*=0) for type IIIB nanodimer relevant to the DDB and DQB modes and Fano resonance

Fig. 14 **a** Sketch of type IV nanodimer. **b** Extinction spectra of type IV nanodimer. Extinction spectra of **c** type IVB and **d** type IVA nanodimers for different values of *G*

Conclusion

We studied theoretically the plasmonic Fano resonance in a dimer based on gold nanocones. By adjusting the geometry parameters, a Fano line shape is observed in the extinction spectrum, which is induced by the interference of bright and dark plasmon modes. Several geometrical configurations have been used to attain Fano resonances. The maximum enhancement for all the types of nanodimer is observed to occur in the gap region between the two nanoparticles. Among all the types, type I arrangement is discovered to provide maximum field enhancement and sharp Fano resonance with greater tunability. However, type IIB nanodimer exhibits a Fano resonance with large modulation depth, typically more capable for PIT application. The plasmonic responses of type IV nanodimer are found to be highly sensitive to the interparticle distance and less affected by the size of the nanoparticle. The results obtained in this work open up the advantageous possibility of using the Fano resonance band for plasmon sensing, PIT, switching, and SERS applications.

References

1. Banaee MG, Crozier KB (2010) Mixed dimer double-resonance substrates for surface-enhanced Raman spectroscopy. Acs Nano 5(1):307–314
2. Cui X, Erni D (2010) The influence of particle shapes on the optical response of nearly touching plasmonic nanoparticle dimers. J Comput Theor Nanosci 7(8):1610–1615
3. Wu DJ, Jiang SM, Cheng Y, Liu XJ (2012) Fano-like resonance in symmetry-broken gold nanotube dimer. Opt Express 20(24):26559–26567
4. Oubre C, Nordlander P (2005) Finite-difference time-domain studies of the optical properties of nanoshell dimers. J Phys Chem B 109(20):10042–10051
5. Yang ZJ, Zhang ZS, Hao ZH, Wang QQ (2011) Fano resonances in active plasmonic resonators consisting of a nanorod dimer and a nano-emitter. Appl Phys Lett 99(8):081103–081107

6. Yang ZJ, Zhang ZS, Zhang LH, Li QQ, Hao ZH, Wang QQ (2011) Fano resonances in dipole–quadrupole plasmon coupling nanorod dimers. Opt Lett 36(9):1542–1544

7. Shao L, Fang C, Chen H, Man YC, Wang J, Lin HQ (2012) Distinct plasmonic manifestation on gold nanorods induced by the spatial perturbation of small gold nanospheres. Nano letters 12(3):1424–1430

8. Brown LV, Sobhani H, Lassiter JB, Nordlander P, Halas NJ (2010) Heterodimers: plasmonic properties of mismatched nanoparticle pairs. Acs Nano 4(2):819–832

9. Wu DJ, Jiang SM, Liu XJ (2012) Fano-like resonances in asymmetric homodimer of gold elliptical nanowires. J Phys Chem C 116(25):13745–13748

10. Liu H, Wu X, Li B, Xu C, Zhang G, Zheng L (2012) Fano resonance in two-intersecting nanorings: multiple layers of plasmon hybridizations. Appl Phys Lett 100(15):153114

11. Xi Z, Lu Y, Yu W, Wang P, Ming H (2013) Improved sensitivity in a T-shaped nanodimer plasmonic sensor. J Opt 15(2):025004

12. Khan AD, Miano G (2013) Higher order tunable Fano resonances in multilayer nanocones. Plasmonics 8(2):1023–1034

13. Khan AD, Miano G (2013) Plasmonic fano resonances in single-layer gold conical nanoshells. Plasmonics. doi:10.1007/s11468-013-9556-4

14. Chao Y-C, Tseng H-C, Chang K-D, Chang C-W (2012) Three types of couplings between asymmetric plasmonic dimers. Opt Express 20(3):2887–2894

15. Zuloaga J, Prodan E, Nordlander P (2009) Quantum description of the plasmon resonances of a nanoparticle dimer. Nano letters 9(2):887–891

16. Schau P, Fu L, Frenner K, Schäferling M, Schweizer H, Giessen H, Gaspar Venancio LM, Osten W (2012) Polarization scramblers with plasmonic meander-type metamaterials. Opt Express 20(20):22700–22711

17. Johnson PB, Christy R (1972) Optical constants of the noble metals. Physl Rev B 6(12):4370–4379

18. Nordlander P, Oubre C, Prodan E, Li K, Stockman M (2004) Plasmon hybridization in nanoparticle dimers. Nano letters 4(5):899–903

19. Grillet N, Manchon D, Bertorelle F, Bonnet C, Broyer M, Cottancin E, Lermé J, Hillenkamp M, Pellarin M (2011) Plasmon coupling in silver nanocube dimers: resonance splitting induced by edge rounding. Acs Nano 5(12):9450–9462

20. He J, Fan C, Wang J, Ding P, Cai G, Cheng Y, Zhu S, Liang E (2013) A giant localized field enhancement and high sensitivity in an asymmetric ring by exhibiting Fano resonance. J Opt 15(2):025007

21. Zhang Y, Jia T, Zhang S, Feng D, Xu Z (2012) Dipole, quadrupole, and octopole plasmon resonance modes in nonconcentric nanocrescent/nanodisk structure: local field enhancement in the visible and near infrared regions. Opt Express 20(3):2924–2931

22. Chen J, Wang P, Chen C, Lu Y, Ming H, Zhan Q (2011) Plasmonic EIT-like switching in bright-dark-bright plasmon resonators. Opt Express 19(7):5970–5978

23. Liusman C, Li H, Lu G, Wu J, Boey F, Li S, Zhang H (2012) Surface-enhanced Raman scattering of Ag–Au nanodisk heterodimers. J Phys Chem C 116(18):10390–10395

24. Jian Y, Pol VD (2012) Nanocrosses with highly tunable double resonances for near-infrared surface-enhanced Raman scattering. Int J Optics 2012. doi:10.1155/2012/745982

25. Dodson S, Haggui M, Bachelot R, Plain Jrm, Li S, Xiong Q Optimizing Electromagnetic Hotspots in Plasmonic Bowtie Nanoantennae. J Phys Chem Lett 4 (3):496–501

26. Sederberg S, Elezzabi A (2011) Nanoscale plasmonic contour bowtie antenna operating in the mid-infrared. Opt Express 19(16):15532–15537

27. Yun B, Wang Z, Hu G, Cui Y (2010) Theoretical studies on the near field properties of nonconcentric core–shell nanoparticle dimers. Opt Commun 283(14):2947–2952